Journal of Magnetism and Magnetic Materials 323 (2011) 1203–1206

Contents lists available at ScienceDirect

Journal of Magnetism and Magnetic Materials

journal homepage: www.elsevier.com/locate/jmmm

$ZnFe_2O_4$ nanoparticles for ferrofluids: A combined XANES and XRD study

J.A. Gomes [a], G.M. Azevedo [b], J. Depeyrot [a,*], J. Mestnik-Filho [c], G.J. da Silva [a], F.A. Tourinho [d], R. Perzynski [e]

[a] Complex Fluids Group, Instituto de Física, Universidade de Brasilia, Caixa Postal 04455, 70919-970 Brasília (DF), Brazil
[b] Departamento de Física, Universidade do Rio Grande do Sul, Caixa Postal 15051, 91501-970 Porto Alegre (RS), Brazil
[c] Instituto de Pesquisas Energéticas e Nucleares, Av. Prof. Lineu Prestes 2242, 05508-000 São Paulo (SP), Brazil
[d] Complex Fluids Group, Instituto de Química, Universidade de Brasilia, Caixa Postal 04478, 70919-970 Brasília-DF, Brazil
[e] Laboratoire PECSA, Université Pierre et Marie Curie, 4 Place Jussieu, 75005 Paris, France

ARTICLE INFO

Available online 25 November 2010

Keywords:
Ferrite magnetic nanoparticle
Cation distribution
X-ray Diffraction
X-ray Absorption Near Edge Spectroscopy (XANES)

ABSTRACT

A soft-chemistry method is used to synthesize zinc ferrite nanoparticles to prepare a magnetic fluid. We investigate here their internal structure by X-ray Absorption Near Edge Spectroscopy (XANES) and X-Ray Diffraction (XRD). A cross analysis of XANES and Rietveld refinement of XRD spectra shows non-equilibrium site occupancy with respect to bulk zinc ferrite, suggesting a cation redistribution that enhances the magnetic and magneto-optical responses of the nanoparticles.

1. Introduction

Among different magnetic materials, spinel ferrite nanoparticles present several advantages that justify their use in biomedical applications [1]. In particular, they can be easily functionalized with biological effectors to make them interact or bind to biological targets. For this purpose, the "soft-chemistry" method has been developed to synthesize nanosized particles of spinel type ferrites dispersible in aqueous media [2].

Spinel ferrites crystallize in a face-centered cubic lattice (Fd3m) formed by a close-packed arrangement of 32 oxygen anions, creating 64 interstices of tetrahedral symmetry (A) and 32 interstices of octahedral symmetry (B) partially occupied by metallic cations. The following crystallographic representation can be used to specify the cation distribution among the tetrahedral and octahedral sites: $[M^{2+}_{(1-x)}Fe^{3+}_{x}]_A[M^{2+}_{x}Fe^{3+}_{2-x}]_BO^{2-}_4$ Here M is a divalent transition metal and x is the inversion degree defined as the fraction of A-sites occupied by Fe^{3+} cations or the fraction of B-sites occupied by M^{2+} cations.

The cation distribution in spinel nanocrystals can modify significantly the saturation magnetization when compared to bulk materials. One of the most studied examples in literature is zinc ferrite, which in ideal bulk crystals presents a normal spinel structure with zinc ions located at tetrahedral sites and iron ions at octahedral sites. Then, ideal zinc ferrite is not magnetic at room temperature. However, the spatial confinement at the nanoscale completely modifies the problem and several works have already shown the existence of a significant magnetic moment of stoichiometric zinc ferrite nanoparticles at room temperature. These findings are usually attributed to a partially inverted structure and the presence of iron ions at tetrahedral sites [3–5]. The inversion degree in redistributed spinels depends on several factors such as, for example, synthesis procedure and spatial confinement at nanoscale as well as nature and size of the cations [6–9]. In stoichiometric zinc ferrite nanocrystals, this non-equilibrium cation distribution among the interstitial sites has been extensively determined using the Rietveld refinement of Neutron Diffraction spectra [4] or X-ray spectra [10], in-field Mössbauer spectroscopy measurements [6,7], Nuclear Magnetic Resonance [11], X-ray Absorption [5,8,9] and X-ray Circular Magnetic Dichroism [12].

The aim of the present work is to synthesize $ZnFe_2O_4$ nanoparticles elaborated in order to perform magnetic nanocolloids [13] and to study their crystalline structure at the local scale. We check here the cation distribution by combining Synchrotron X-Ray Absorption Near Edge Spectroscopy (XANES) and X-Ray Diffraction (XRD) experiments.

2. Experimental methods and computational procedure

2.1. Chemical synthesis

The spinel $ZnFe_2O_4$ nanoparticles are prepared by hydrothermal coprecipitation at 100 °C, alkalinizing 1:2 mixtures of Zn^{2+} and Fe^{3+} with NaOH under vigorous stirring. Thanks to a protective surface treatment, the coprecipitated nanoparticles are then dispersed in an acidic medium. The resulting magnetic liquids present, at room temperature, gigantic magnetic [14] and magneto-optical [15] responses when an external field is applied. At each step of the synthesis, the Fe^{3+} and Zn^{2+} contents in the

* Corresponding author. Tel./fax: +55 61 33072900.
E-mail address: depeyrot@fis.unb.br (J. Depeyrot).

0304-8853/$ - see front matter © 2010 Published by Elsevier B.V.
doi:10.1016/j.jmmm.2010.11.006

nanoparticles are determined by inductively coupled plasma atomic emission. The nanoparticles investigated here are obtained soon after the coprecipitation step, not yet surface treated, and are stoichiometric, the molar fraction of divalent metal being 0.33. Moreover, the $ZnFe_2O_4$ reference compound has been obtained using a hard chemical route.

2.2. X-ray Absorption Near Edge Spectroscopy measurements (XANES)

XANES spectra are collected in transmission mode, at 20, 150 and 300 K, at the D04B-XAFS1 beam line [16] of the Brazilian synchrotron (LNLS) around the Fe and Zn K-edges. Each spectrum corresponds to an average over three independent scans. The spectra are calibrated in energy by simultaneous measurements of transmission spectra of Fe and Zn foils. The energies E_0 of the first inflection point at the absorption edge of these reference samples are, respectively, 7112 and 9662 eV.

2.3. X-ray powder diffraction

X-ray powder diffraction data (XPD) are collected at room temperature at the D12A-XRD beam line of the Brazilian Synchrotron Light Laboratory (LNLS), using a double crystal Si(1 1 1) monochromator with constant offset, a graphite (0 0 2) analyzer and a scintillation counter as detector. Samples are placed in a cylindrical sample holder that is spun during data collection in order to minimize effects of an eventual preferential orientation. The measurements are performed with a monochromatic X-ray beam, $\lambda = 2.0633$ Å (6.01 keV), with an approximate area of 4×1.5 mm^2. Diffraction patterns are obtained typically within a $20^\circ \leq 2\theta \leq 130^\circ$ interval scanned with an angle step of 0.04°.

Rietveld structure refinement of the XPD data is performed using the GSAS software package developed by Larson and Von Dreele [17]. It provides a fitting procedure of experimental results and allows one to determine here the lattice parameter, oxygen position and cation distribution. The structure refinements are made with a peak shape modeled by a pseudo-Voigt function that includes a correction for peak asymmetry and background intensity well accounted by a Chebyshev polynomial function. Each diffractogram is fitted until convergence, the best result being selected on the basis of reliability factor of refinement (R_{wp}) and quality of fit (χ^2).

3. Results and discussion

3.1. X-rayAbsorption Near Edge Spectroscopy measurements (XANES)

Fig. 1 displays experimental the XANES spectra at Zn K-edge for bulk zinc ferrite and nanocrystalline sample. Let us focus on some distinct features in the bulk spectrum: three peaks just above the edge, located at 9663, 9667 and 9671 eV, and a shoulder centered at 9675 eV. The spectra of nanoparticles exhibit the same three peaks, more intense than in the bulk spectrum, and the shoulder is absent. Such behavior is ascribable to cation inversion in the nanoparticles structure, as checked by simulations of the absorption spectrum. These calculations have been performed in order to verify if the behavior observed in our coprecipitated nanoparticles, compares well with those concluded by others authors, in ball-milled nanoparticles [8]. Full Multiple Scattering (FMS) and Self Consistent Field (SCF) XANES calculations are performed using the FEFF 8.4 code [18] for bulk Zn ferrite structures with increasing inversion degrees. A cluster including all atoms within a sphere of 20 Å (390 atoms) is used in the calculations. Self-consistency is calculated within a cluster of 7 Å and Full Multiple Scattering within a radius

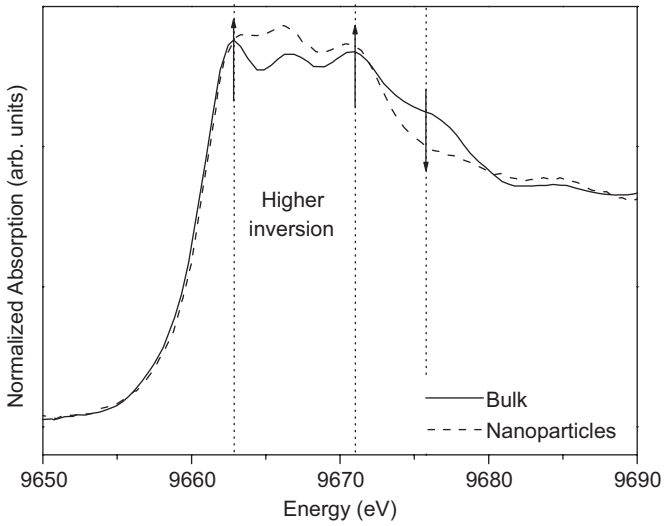

Fig. 1. Experimental XANES spectrum at Zn K-edge, for zinc ferrite bulk material and nanoparticle samples.

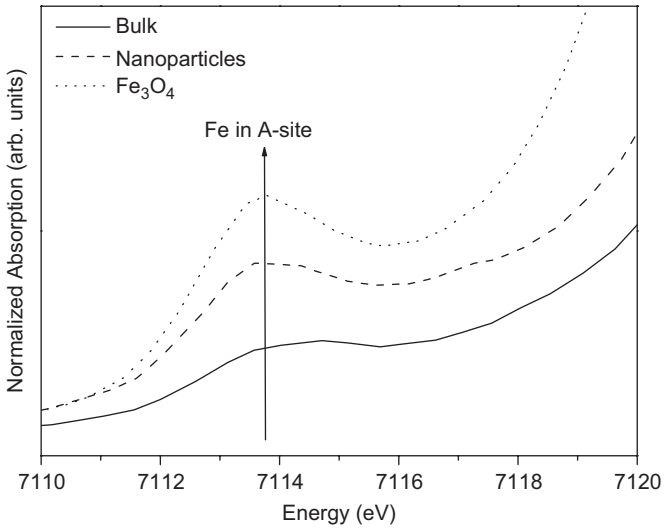

Fig. 2. "Pre-edge" resonances of the experimental XANES spectrum, at Fe K-edge, for zinc ferrite, Fe_3O_4 bulk material and nanoparticles samples.

of 10 Å. The ION card is used (ION = 02) meaning a total charge of +2 is located at the central atom. The results indicate that as the inversion degree increases, the intensities of the first and the third peaks just above the edge increase as well, while the second one remains unchanged and shoulder intensity diminishes. Such a behavior is in good agreement with the results reported in Ref. [8], in which similar SCF and FMS parameters with the so-called "Z+1 approximation" for calculation of bulk $ZnFe_2O_4$ absorption spectra were used. It therefore shows unambiguously the presence of Zn^{2+} ions at octahedral sites of the synthesized nanoparticles.

Fig. 2 shows a magnification of the pre-edge region of the room temperature XANES spectra obtained at Fe K-edge with reference compounds and nanoparticles. The small peak around 7115 eV is associated with the contributions of both electronic $1s \rightarrow 3d$ quadrupole transition and $1s \rightarrow 3d/4p$ dipole transition [8].

The intensity of the pre-peak mainly depends on the local symmetry and also on the ion valence, even if it is in a minor scale: (i) it is very low for common octahedral sites whereas cations localized at tetrahedral sites give rise to a pre-peak of high intensity and (ii) the greater the metal valence, the larger the pre-peak

intensity. In this context, the pre-peak observed in the magnetite spectrum is intense since Fe_3O_4 possesses a larger amount of iron ions at tetrahedral sites. On the contrary, in bulk zinc ferrite, Fe^{3+} ions are located only at octahedral sites and the intensity of the pre-peak is low. Nanoparticle samples have an intensity that varies between the values of bulk Fe_3O_4 and bulk $ZnFe_2O_4$. Thus, it shows a distribution of iron ions at tetrahedral and octahedral sites, clearly different from that of bulk zinc ferrite, in which there is no Fe^{3+} ion at tetrahedral sites. In the zinc ferrite nanocrystals some of the Fe^{3+} ions are located at tetrahedral sites.

3.2. X-ray powder diffraction (XPD)

Using Bragg's Law the diffraction peaks are indexed and associated with the interplane spacings of only one crystalline phase, which corresponds to the spinel structure, in both $ZnFe_2O_4$ bulk and nanoparticles samples. The profile of X-ray diffraction data is fitted using the Rietveld analysis and the corresponding indexed spectra are typically displayed in Fig. 3 for nanoparticle samples. Both of the resulted weighted profile reliability factors $R_{wp}=5.3\%$ and $\chi^2=2.7$ indicate a good agreement between the data and the structural model. Here, in addition to the peak shape parameters and its broadening due to particle size, the refined parameters are the size of the spinel cubic cell, oxygen position and inversion degree. For the latter, the condition was imposed that the quantity of iron ions migrating from B-sites to A-sites is the same as the quantity of zinc ions migrating in reverse order.

The nanoparticles mean size deduced from the refinement of the diffracted intensity profile is 9.6 nm. The lattice parameter is found to be equal to 8.430(1) Å, in good agreement with the standard ASTM value of 8.441 Å (ASTM—file 22-1012). The resulting oxygen position is 0.253(1) and it does not correspond exactly to a perfect compact packing since it slightly differs from the ideal value of 0.25. This observation seems to be common with the spinel structure of ferrites due to the size mismatch of metallic cations, which could induce a slight distortion of the oxygen positions [4]. The value found for the inversion degree, $x=0.33(2)$, unambiguously shows that the nanoparticles present a distribution character of inverted metallic cations.

For comparison with a nanomaterial the Rietveld method has been applied to the spectrum of bulk reference material. The value of density has been found to be equal to 5.320 g/cm^3, well comparable to the ideal value of 5.324 g/cm^3. The quality factors values of refinement obtained after data convergence were $R_{wp}=6.43\%$ and $\chi^2=2.176$. Structural parameter values determined by the Rietveld refinement were 8.4436 ± 0.0001 Å for the lattice parameter, 0.2587 ± 0.0005 for the oxygen position and 0.00 ± 0.02 for the inversion degree, very close to the ideal (normal spinel) values, which are $a=8.4411$ Å, $u=0.25$ and $x=0$.

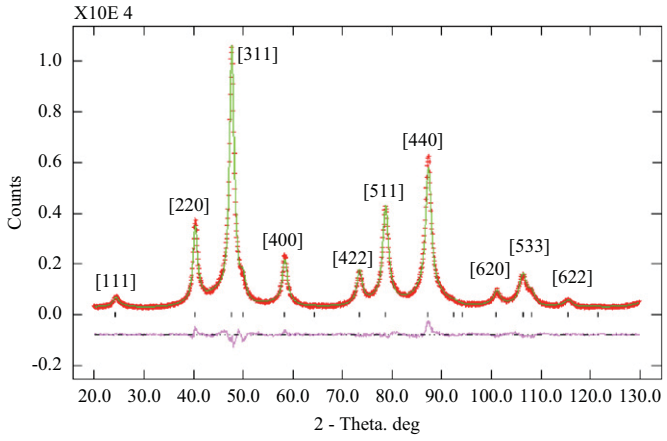

Fig. 3. The Rietveld refinement pattern for nanoparticles sample. X-ray data are shown by +marks; the solid line is the best fit to the data and the tick marks show the positions of the allowed reflections. The lower curve represents the difference between observed and calculated profiles.

In literature, the occurrence of partial inversion appears to be strongly dependent on the method used to prepare the $ZnFe_2O_4$ nanomaterial. Methods that use high temperature treatment generally lead to the ideal normal spinel structure whereas high energy ball milling, mechanochemistry and soft chemical routes induce a non-equilibrium cation distribution among the interstitial sites. For the coprecipitated nanoparticles investigated here, the value found for the inversion degree by fitting experimental XRD data compares well with others values relative to nanocrystals obtained by soft chemical routes [3,8,10]. Such cation redistribution therefore confirms the existence of an enhanced magnetic moment, which is responsible for the observed magnetic and magneto-optical behaviors of Ref. 13–15.

4. Summary

Due to the close connection between the magnetic properties and the crystal structure, a clear understanding of the internal nanoparticles atomic arrangement is essential to control their magnetic properties. It has been possible to study the non-equilibrium site occupancy in zinc ferrite nanoparticles, by crossing two independent analyses of XANES and Rietveld refinement of X-ray Diffraction patterns. On the whole it suggests a non-equilibrium cation distribution among interstitial sites of the structure that enhances the magnetic response of the nanoparticles. Fitting the experimental XRD data provided an inversion degree equal to 0.33. In the near future, it would be interesting to investigate the effect of surface treatment used to thermodynamically stabilize the nanoparticles in a liquid acid medium on local structure. Moreover, the inversion degree would be evaluated from the EXAFS data and magnetization measurements performed at low temperatures.

Acknowledgements

This work was supported by the Brazilian agencies FAP/DF, FINATEC, FAPESP and CNPq. The authors are also greatly indebted to LNLS for beam-time obtained on D12A-XRD1 beam-line (X-ray Diffraction) and D04B-XAFS1 beam-line (X-ray Absorption). We greatly acknowledge the CAPES–COFECUB French–Brazilian cooperation program and also thank M.H. Sousa for technical assistance.

References

[1] Q.A. Pankhurst, N.K.T. Thanh, S.K. Jones, J. Dobson, J. Phys. D 42 (2009) 224001.
[2] F.A. Tourinho, R. Franck, R. Massart, J. Mater. Sci. 25 (1990) 3249.
[3] T. Sato, K. Haneda, M. Seki, T. Iijima., Appl. Phys. A 50 (1990) 13.
[4] T. Kamiyama, K. Haneda, T. Sato, S. Ikeda, H. Asano., Solid State Commun. 81 (1992) 563.
[5] B. Jeyadevan, K. Tohji, K. Nakatsuka, J. Appl. Phys. 76 (1994) 6325.
[6] C.N. Chinnasamy, A. Narayanasamy, N. Ponpandian, K. Chattopadhyay, H. Guérault, J.M. Grenèche, J. Phys.: Condens. Matter 12 (2000) 7795.
[7] S. Ammar, N. Jouini, F. Fiévet, Z. Beji, L. Smiri, P. Moliné, M. Danot, J.M. Grenèche, J. Phys.: Condens. Matter 18 (2006) 9055.
[8] S.J. Stewart, S.J.A. Figueroa, J.M. Ramallo Lopez, S.G. Marchetti, J.F. Bengoa, R.J. Prado, F.G. Requejo, Phys. Rev. B 75 (2007) 073408.
[9] S. Nakashima, K. Fujita, K. Tanaka, H. Kazuyuki, T. Yamamoto, I. Tanaka, Phys. Rev. B 75 (2007) 174443.
[10] H.H. Hamdeh, J.C. Ho, S.A. Oliver, R.J. Willey, G. Oliveri, G. Busca, J. Appl. Phys. 81 (1997) 1851.
[11] J.H. Shim, S. Lee, J.H. Park, S.J. Han, Y.H. Jeong, Y.W. Cho, Phys. Rev. B 73 (2006) 064404.
[12] S. Ammar, N. Jouini, F. Fiévet, O. Stephan, C. Marhic, M. Richard, F. Villain, C. Cartier dit Moulin, S. Brice, P. Sainctavit, J. Non-Cryst. Solids 345–346 (2004) 658.

[13] J.A. Gomes, M.H. Sousa, F.A. Tourinho, R. Aquino, G.J. da Silva, J. Depeyrot, J.E. Dubois, R. Perzynski, J. Phys. Chem. C 112 (2008) 6220.
[14] M.H. Sousa, F.A. Tourinho, J. Depeyrot, G.J. da Silva, M.C.F.L. Lara, J. Phys. Chem. B 105 (2001) 1168.
[15] J. Depeyrot, G.J. da Silva, C.R. Alves, E.C. Sousa, M. Magalhães, A.M. Figueiredo Neto, M.H. Sousa, F.A. Tourinho, Braz. J. Phys. 31 (2001) 390.
[16] H.C.N. Tolentino, A.Y. Ramos, M.C.M. Alves, R.A. Barrea, E. Tamura, J.C. Cezar, N. Watanabe, J. Synchrotron Radiat. 8 (2001) 1040.
[17] C. Larson, R.B. Von Dreele, General structure analysis system, Los Alamos National Laboratory, 2001, 〈ftp://ftp.lanl.gov/public/gsas〉.
[18] A.L. Ankudinov, B. Ravel, J.J. Rehr, S.D. Conradson, Phys. Rev. B 58 (1998) 7565.